REPORT DOCUMENTATION PAGE

Form Approved OMB NO. 0704-0188

The public reporting burden for this collection of information is estimated to average 1 hour per response, including the time for reviewing instructions, searching existing data sources, gathering and maintaining the data needed, and completing and reviewing the collection of information. Send comments regarding this burden estimate or any other aspect of this collection of information, including suggesstions for reducing this burden, to Washington Headquarters Services, Directorate for Information Operations and Reports, 1215 Jefferson Davis Highway, Suite 1204, Arlington VA, 22202-4302. Respondents should be aware that notwithstanding any other provision of law, no person shall be subject to any oenalty for failing to comply with a collection of information if it does not display a currently valid OMB control number.
PLEASE DO NOT RETURN YOUR FORM TO THE ABOVE ADDRESS.

1. REPORT DATE (DD-MM-YYYY)	2. REPORT TYPE	3. DATES COVERED (From - To)
08-06-2010	Final Report	15-Aug-2007 - 14-Feb-2010

4. TITLE AND SUBTITLE	5a. CONTRACT NUMBER
Atom Interferometry on Atom Chips - A Novel Approach Towards Precision Inertial Navigation System - PINS	W911NF-07-1-0496
	5b. GRANT NUMBER
	5c. PROGRAM ELEMENT NUMBER
	7D10Q6

6. AUTHORS	5d. PROJECT NUMBER
Vladan Vuletic, Mara Prentiss	5e. TASK NUMBER
	5f. WORK UNIT NUMBER

7. PERFORMING ORGANIZATION NAMES AND ADDRESSES	8. PERFORMING ORGANIZATION REPORT NUMBER
Massachusetts Institute of Technology Office of Sponsored Programs Bldg. E19-750 Cambridge, MA 02139 -4307	

9. SPONSORING/MONITORING AGENCY NAME(S) AND ADDRESS(ES)	10. SPONSOR/MONITOR'S ACRONYM(S)
U.S. Army Research Office P.O. Box 12211 Research Triangle Park, NC 27709-2211	ARO
	11. SPONSOR/MONITOR'S REPORT NUMBER(S)
	53021-PH-DRP.1

12. DISTRIBUTION AVAILIBILITY STATEMENT

Approved for Public Release; Distribution Unlimited

13. SUPPLEMENTARY NOTES

The views, opinions and/or findings contained in this report are those of the author(s) and should not contrued as an official Department of the Army position, policy or decision, unless so designated by other documentation.

14. ABSTRACT

We have proposed and experimentally demonstrated a new technique for creating spin squeezed states of distant atoms by their common interaction with a driven resonator mode. Using this technique we achieve the largest spin squeezing to date, 5.6dB of improvement in signal-to-noise ratio over the standard quantum limit. We have demonstrated a squeezed atomic clock that reaches a given precision a factor of 2.8 faster than a clock operating at the standard quantum limit. Furthermore we have experimentally demonstrated that an atom-optics kicked rotor can

15. SUBJECT TERMS

Atom interferometry, quantum mechanical many-body states, spin squeezing

16. SECURITY CLASSIFICATION OF:			17. LIMITATION OF ABSTRACT	15. NUMBER OF PAGES	19a. NAME OF RESPONSIBLE PERSON
a. REPORT	b. ABSTRACT	c. THIS PAGE	UU		Vladan Vuletic
UU	UU	UU			19b. TELEPHONE NUMBER 617-324-1174

Atom Interferometry on Atom Chips - A Novel Approach Towards Precision Inertial Navigation System - PINS

ABSTRACT

We have proposed and experimentally demonstrated a new technique for creating spin squeezed states of distant atoms by their common interaction with a driven resonator mode. Using this technique we achieve the largest spin squeezing to date, 5.6dB of improvement in signal-to-noise ratio over the standard quantum limit. We have demonstrated a squeezed atomic clock that reaches a given precision a factor of 2.8 faster than a clock operating at the standard quantum limit. Furthermore we have experimentally demonstrated that an atom-optics kicked rotor can remove the interference signal due to chosen interferometer paths in a four-pulse atom interferometer. The interferometer output is dominated by two degenerate spatial loops: the nonreciprocal "trapezoid" loop and the reciprocal "figure-8" loop. By applying the kicked rotor sequence at a particular time we suppressed the contribution of the "trapezoid" loop to the interferometer signal while preserving the contribution due to the "figure-8" loop. We have also demonstrated a robust "macro-chip" as a guide for stationary interferometer and investigated the properties of such interferometer.

List of papers submitted or published that acknowledge ARO support during this reporting period. List the papers, including journal references, in the following categories:

(a) Papers published in peer-reviewed journals (N/A for none)

1.   J. Simon, H. Tanji, J. K. Thompson, and V. Vuletic, Interfacing Collective Atomic Excitations and Single Photons, Phys. Rev. Lett. 98, 183601 (2007).
2.   Single-Photon Bus between Spin-Wave Quantum Memories. J. Simon, H. Tanji, S. Ghosh, and V. Vuletic, Nature Physics 3, 765-769 (2007).
3.   Wu S, Su E, Prentiss M, Demonstration of an area-enclosing guided-atom interferometer for rotation sensing, Phys. Rev. Lett. 99, 173201 (2007).
4.   Heralded Single-Magnon Quantum Memory for Photon Polarization States. H. Tanji, S. Ghosh, J. Simon, B. Bloom, and V. Vuletic, Phys. Rev. Lett. 103, 043601 (2009); selected as Editors' Suggestion, accompanying Viewpoint commentary Physics 2, 62 (2009).
5.   Heralded atomic-ensemble quantum memory for photon polarization states. J. Simon, H. Tanji, S. Ghosh, B. Bloom, and V. Vuletic, Phys. Scr. T134, 014010 (2009).
6.   Selective Manipulation of Degenerate Interferometer Loops by an Atom-Optics Kicked Rotor. A. Tonyushkin and M. Prentiss, Phys. Rev. A 78, 053625 (2008).
7.   Demonstration of multipulse interferometer for quantum kicked-rotor studies. A. Tonyushkin, S. Wu, and M. Prentiss, Phys. Rev. A 79, 051402(R) (2009); selected to Virtual Journal of Ultrafast Science, 8 (6).
8.   Observation of saturation of fidelity decay with an atom interferometer. S. Wu, A. Tonyushkin, and M. Prentiss, Phys. Rev. Lett. 103, 034101 (2009).
9.   Implementation of Cavity Squeezing of a Collective Atomic Spin. I.D. Leroux, M. Schleier-Smith, and V. Vuletic, Phys. Rev. Lett. 104, 073602 (2010); selected as Editors' Suggestion.
10. States of an Ensemble of Two-Level Atoms with Reduced Quantum Uncertainty. M. H. Schleier-Smith, I.D. Leroux, and V. Vuletic, Phys. Rev. Lett. 104, 073604 (2010).
11. Squeezing the Collective Spin of a Dilute Atomic Ensemble by Cavity Feedback. M. Schleier-Smith, I.D. Leroux, and V. Vuletic, Phys. Rev. A 81, 021804(R) (2010).

Number of Papers published in peer-reviewed journals: 11.00

(b) Papers published in non-peer-reviewed journals or in conference proceedings (N/A for none)

1.   Simplified measurement of the Bell parameter of two photons within quantum mechanics. H. Tanji, J. Simon, S. Ghosh, and V. Vuletic, quant-phys/08014549 (1/2008).
2.   Nonclassical States of Cold Atomic Ensembles and of Light Fields. V. Vuletic, RLE Progress Report 149, Chapter 35 (2008).
3.   Observation of coherence revival and fidelity saturation in a delta-kicked rotor potential. S. Wu, A. Tonyushkin, M. Prentiss, arXiv:0801.0475.

Number of Papers published in non peer-reviewed journals: 3.00

(c) Presentations

about 15 presentations

Number of Presentations: 15.00

Non Peer-Reviewed Conference Proceeding publications (other than abstracts):

1. Spin Squeezing on an Atomic Clock Transition. M. H. Schleier-Smith, I. D. Leroux, and V. Vuletic, published in: Proceedings of the XXI. International Conference on Atomic Physics (ICAP 2008, Storrs, Connecticut, 7/2008), edited by R. Côté, P.L Gould, M. Rozman, and W.W. Smith (World Scientific 2009).

Number of Non Peer-Reviewed Conference Proceeding publications (other than abstracts):   1

Peer-Reviewed Conference Proceeding publications (other than abstracts):

1. Probing quantum chaos with periodically perturbed de Broglie wave atom interferometer. A. Tonyushkin and M. Prentiss, published in: Proceedings of International Laser Physics Workshop. Barcelona, Spain (Jul, 2009).
2. Spin Squeezing on an Atomic Clock Transition. M. H. Schleier-Smith, I. D. Leroux, and V. Vuletic, published in: Proceedings of the XXI. International Conference on Atomic Physics (ICAP 2008, Storrs, Connecticut, 7/2008), edited by R. Côté, P.L Gould, M. Rozman, and W.W. Smith (World Scientific 2009).
3. Coherence modulation at quantum resonances of delta-kicked rotor. A. Tonyushkin, M. Hafezi, S. Wu, and M. Prentiss, published in: Proceedings of the XXI. International Conference on Atomic Physics (ICAP 2008, Storrs, Connecticut, 7/2008), edited by R. Côté, P.L Gould, M. Rozman, and W.W. Smith (World Scientific 2009).
4. Perfect Coherence Preservation in an Atom Interferometer Perturbed by Optical Standing Wave Pulses Acting as a Kicked Rotor. A. Tonyushkin, S. Wu, and M. Prentiss, proceedings of Conference on Lasers and Electro-Optics/Quantum Electronics and Laser Science Conference, San Jose, CA (2008), Technical Digest (OSA, Washington, DC, 2008)
5. Observation of Fidelity Saturation in a ?-Kicked Rotor Potential. S. Wu, A. Tonyushkin, and M. Prentiss, proceedings of Conference on Lasers and Electro-Optics/Quantum Electronics and Laser Science Conference, San Jose, CA (2008), Technical Digest (OSA, Washington, DC, 2008)

Number of Peer-Reviewed Conference Proceeding publications (other than abstracts):   5

(d) Manuscripts

Number of Manuscripts: 0.00

Patents Submitted

Patents Awarded

Graduate Students

NAME	PERCENT_SUPPORTED
Haruka Tanji	0.50
Ian Leroux	0.50
FTE Equivalent:	**1.00**
Total Number:	**2**

Names of Post Doctorates

NAME	PERCENT_SUPPORTED
Alexey Tonyushkin	1.00
FTE Equivalent:	**1.00**
Total Number:	**1**

Names of Faculty Supported

NAME	PERCENT_SUPPORTED	National Academy Member
Mara Prentiss	0.30	No
Vladan Vuletic	0.30	No
FTE Equivalent:	**0.60**	
Total Number:	**2**	

Names of Under Graduate students supported

NAME	PERCENT_SUPPORTED
Wathid Assawasunthonnet	0.75
Benjamin Bloom	0.50
Thaned Pruttivarasin	0.50
Adele Schwab	0.25
Alexander Papageorge	0.25
Tracy Li	0.50
Xingze (Ken) Wang	0.25
FTE Equivalent:	**3.00**
Total Number:	**7**

Student Metrics
This section only applies to graduating undergraduates supported by this agreement in this reporting period

The number of undergraduates funded by this agreement who graduated during this period: 5.00

The number of undergraduates funded by this agreement who graduated during this period with a degree in science, mathematics, engineering, or technology fields:····· 5.00

The number of undergraduates funded by your agreement who graduated during this period and will continue to pursue a graduate or Ph.D. degree in science, mathematics, engineering, or technology fields:····· 4.00

Number of graduating undergraduates who achieved a 3.5 GPA to 4.0 (4.0 max scale): 5.00

Number of graduating undergraduates funded by a DoD funded Center of Excellence grant for Education, Research and Engineering: 0.00

The number of undergraduates funded by your agreement who graduated during this period and intend to work for the Department of Defense 0.00

The number of undergraduates funded by your agreement who graduated during this period and will receive scholarships or fellowships for further studies in science, mathematics, engineering or technology fields: 3.00

Names of Personnel receiving masters degrees

NAME
Total Number:

Names of personnel receiving PHDs

NAME
Yu-ju Lin
Total Number: **1**

Names of other research staff

NAME   <u>PERCENT SUPPORTED</u>

FTE Equivalent:
Total Number:

Sub Contractors (DD882)

Inventions (DD882)

<u>NAME</u>   <u>PERCENT SUPPORTED</u>

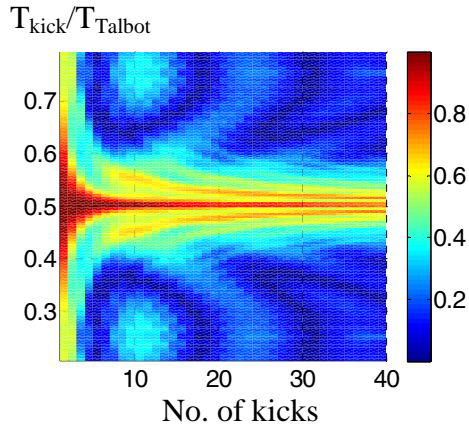**FTE Equivalent:**
Total Number:

Sub Contractors (DD882)

Scientific progress and accomplishments

Prentiss group

1.   Study of coherence dynamics in an atom interferometer perturbed by a delta kicked rotor

An atom optics delta kicked rotor (ADKR) has proved to be a rich tool to study dynamics of quantum coherences and underlying classical dynamics in quantum systems. In our experiment we subject a cloud of cold rubidium atoms in a magnetic guide to periodic kicks from a sinusoidal potential created by a standing wave pulses of off-resonant laser light. We observed matter-wave coherence revivals at a high number of kicks and large kicking strength corresponding to a classical chaos for the exact quantum resonance conditions of the ADKR. We also found that there exist very robust conditions independent on the number of kicks and strength that perfectly preserve coherence.

The coherence is perfectly preserved when the kicking period is equal to rational fraction of the inverse atomic recoil frequency, independent of the strength, amplitude noise and number of kicks applied during one interferometer cycle. This demonstration of perfect coherence preservation in a system that strongly perturbed by a pulsed optical lattice may have important implications for experiments which use entangled states, including quantum computers, that are at present limited by decoherence.

T_{kick}/T_{Talbot}

Figure P1. Perfect coherence preservation at resonance kicking period $T_{kick}/T_{Talbot}=0.5$ **(simulations)**

No. of kicks

We showed that the decoherence between matter-waves in different arms of the interferometer is related to quantum *fidelity* decay under a momentum displacement perturbation [23]. We demonstrated experimentally that when a few kicks are applied, the perturbation nearly destroys the coherence in the interferometer; however, the coherence

revives and approaches a finite asymptote as the number of applied kicks increases. In addition, in our work we showed that the narrowing of the width of coherence revival as a function of increasing kick number and power provides a new technique for accurate measurement of the recoil frequency.
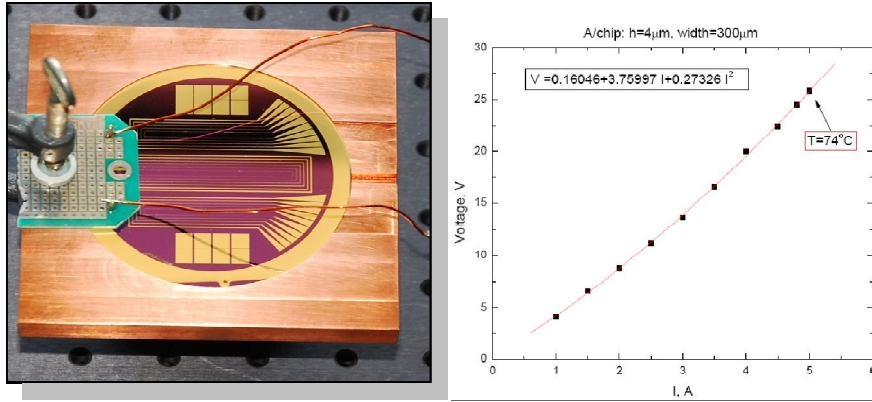

Figure P2: Dephasing factor f at $T_{kick} = 0.5$. Scatter plots give experimental data. Solid lines are calculated according to theory f vs N.

2.   Multi-wire atom chip for guided atom gyroscope

For rotation sensing application of the atom interferometers the paths of the guided atoms must enclose area. This can be achieved using a curved guide [24] or a straight magnetic guide if the two wave-packets follow different paths [25-26]. The sensitivity of the gyroscope increases with the area enclosed according to the Sagnac effect; therefore, it is desirable to create compact interferometers that enclose large areas. This task can be implemented by splitting the atom wave-packets along the guiding direction and then translating the position of the guide to enclose area, where the atoms can follow reciprocal paths that greatly reduce decoherence due to time independent variations in the guiding potential [27]. Such reciprocal paths can also go around the same physical area many times resulting in enclosed sensing area that can be much larger than the physical area of the device. The magnetic guide can be transported by moving the guiding structure [26], but the constraints on the physical motion are substantial; therefore, it is desirable to keep the position of the guiding structure fixed while translating the position
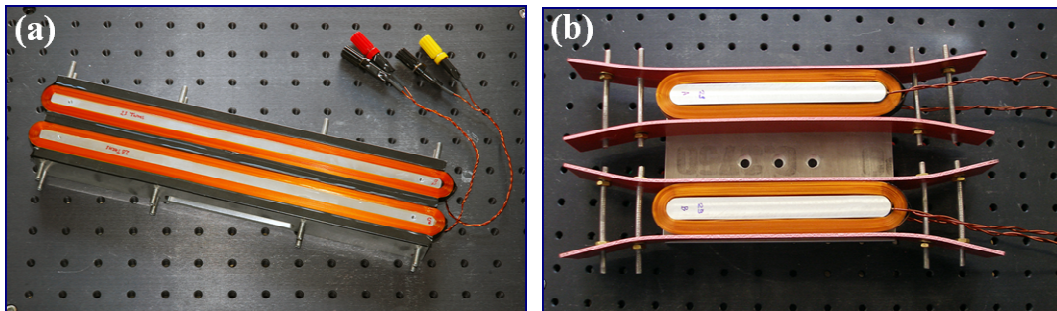
of the guiding potential by using time-dependent currents. Chip-based geometries using 50 micron scale wires are capable of transporting atom micro-traps over mm distance [28] and can potentially achieve smooth cm scale translations of atom guides [29].

Figure P3. Multi-wire atom test chip fabricated in collaboration with AFRL (*Hanscom)* for smooth translation of guided atoms and enclose the area. *V (I)* characteristic curve showing near-linear regime for current up to 5 A in CW mode.

Here, we have designed and fabricated such a multiple wire atom chip (Fig.P3), which should allow smooth translation of guided atoms while enclosing the area for rotation sensitive measurements. Tests in open air CW current regime showed that the chip can withstand currents of up to 5 A, higher current can be also applied at pulsed regime. That performance can potentially be achieved *in-situ* without additional thermal cooling, which is crucial for actual devices.

3. Macroscopic magnetic guiding structures for atom interferometer
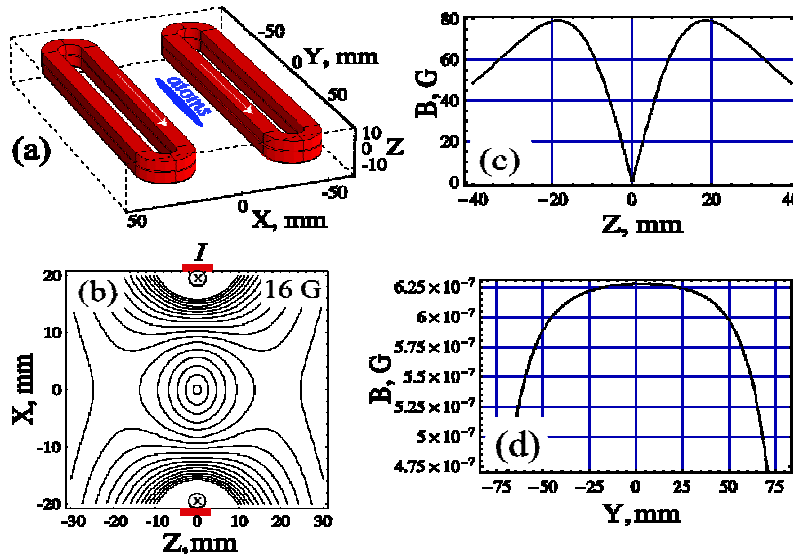

Figure P4. Macroscopic guiding structures a) regular counter-propagating current geometry; b) symmetric co-propagating current geometry.
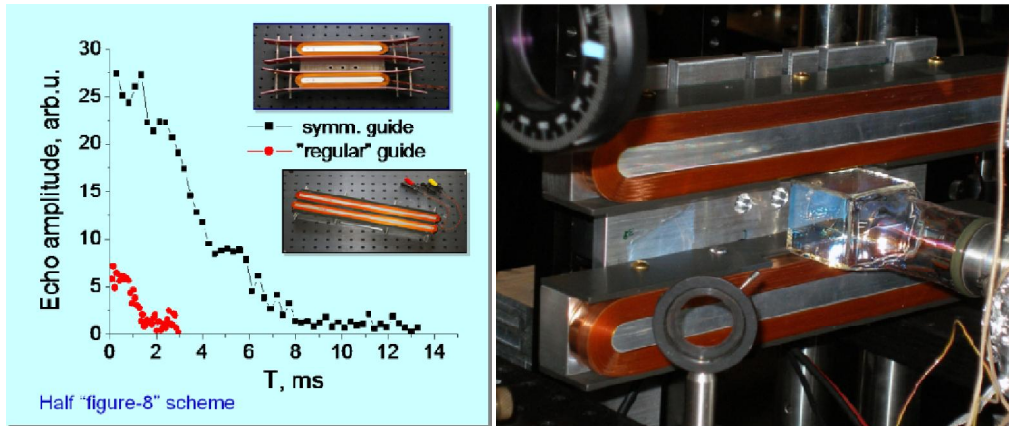
Presently, the most common type of magnetic guides for neutral atoms is micro-fabricated structures on dielectric substrates. Due to requirements on the potential smoothness, such a guide needs to be fabricated with submicron precision, which is still considered a challenge. Because of field enhancement in ferro-foils the operational distance can be large; however, the hysteretic nature of ferromagnetic materials does not allow precise control over the magnetic field.

We have demonstrated a new symmetric current carrying structure (Fig P4b) that results in extremely low curvature in a device whose length is of the same order as its transverse size (Fig. P5). We also show that a comparable non-symmetric guide has more than five orders of magnitude larger curvature essentially providing a weak harmonic confinement of atoms. In our symmetric geometry the edge effects are significantly suppressed resulting in a 10^{-8} ratio of the gradients along the longitudinal and the transverse direction, respectively, over the 90% of the length. Our macroscopic guide is based on parallel co-propagating current in a co-planar guiding geometry, which was previously demonstrated for a microscopic chip. The symmetric macro-guide was used to make an atom interferometer with cold atoms (Fig P5A).

Figure P5. Symmetric guide configuration (a), and magnetic field of the guide for current of 50 A: (b) contour plot of the magnetic field vs position (x,z) (the separation between the lines is 16G, the tape conductors from two coils and direction of the current are shown for the reference); (c) magnetic field vs x; (d) magnetic field vs y, which gives the curvature of the field near the axis.

We have also built an improved version of symmetric macro-guide. We obtained an interferometer signal from new guide. We have incorporated an advanced closed loop optical alignment system for fine tuning the optical beams with respect to guide axis. Further developments may include symmetric permanent magnet and ferromagnetic guides capable of smooth guide translation over the macroscopic distance.
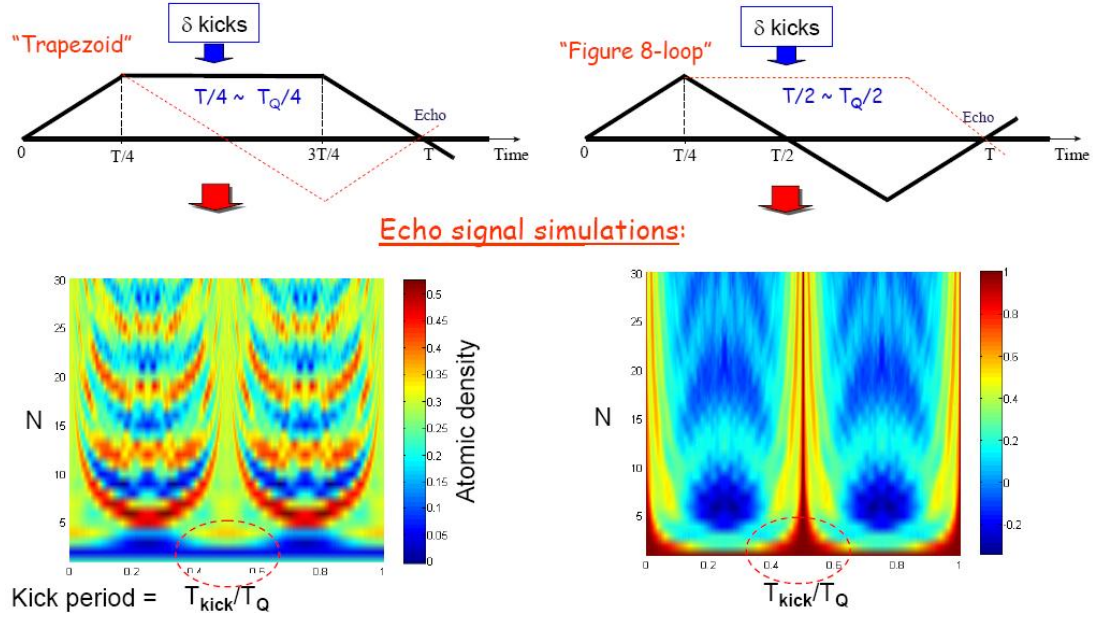

Figure P5A. 3-pulse echo data for interferometer with macroscopic regular and symmetric geometry guides a); improved version of symmetric macro-chip b).

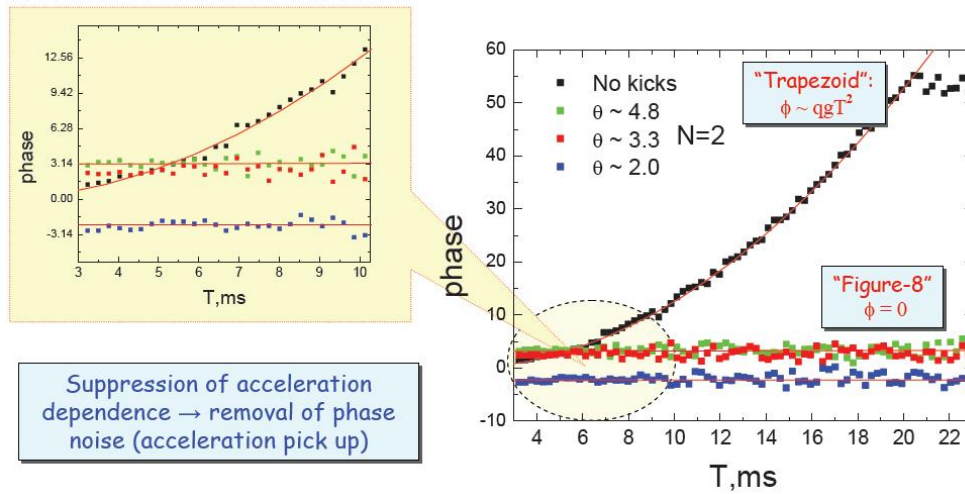4. **Manipulation of degenerate interferometer loops by an atom-optics kicked rotor**

In previous work [54,55] we found new regimes that perfectly preserve coherence of our interferometer independent on the number and the strength of the pulses applied. It would allow us to apply the interferometry sequence N times and correspondingly increase the area and the gyroscope sensitivity by factor of N. These new results also lead to a development of a new technique for selective manipulation of a generate loops in atom interferometer. We used this technique to demonstrate that the non-reciprocal loop can be suppressed degenerate loops in atom interferometer. By eliminating the degenerate loops alone we expect to increase the resolution of the gyroscope by a factor of two.

Our demonstration of the method is a very important result that shows the suppression of the nonreciprocal loop at any time window including a very short interrogation time, where the signal-to-noise ratio for the total amplitude is the highest. That allows us to use the scheme for high bandwidth inertial sensing. The technique can

very effectively be used to elevate stringent requirements on the angle alignment of optical beams in the horizontal plane if one wants to cancel gravity impact.

Figure P6. Effect of "kicked-rotor" (KR) perturbation on two major degenerate loops of balanced 4-pulse interferometer scheme: "Figure-8" and "Trapezoid". At certain time of KR application the signal from Trapezoid loop is suppressed while Figure-8 loop survives.

Figure P7. Demonstration of Trapezoid loop suppression due to KR at different strength θ. The demonstrated phase resolution improvement is 1.25, due to presence of additional phase noise for single shot; averaging would give factor of 2.

Vuletic group

5. Heralded quantum memory for photon polarization states

A quantum memory [1-3], i.e. a device for storing and retrieving quantum states, is a key element of any quantum information processor. Optical memory access is highly desirable, since it is intrinsically fast, and single photons are robust, easily controlled carriers of quantum states. While a bit of quantum information (qubit) can be stored in a single two-level system, e.g. a single atom, it can be expedient to instead use long-lived collective spin excitations of an atomic ensemble. The ensemble can then be viewed as a "macro-atom" whose excitations are quantized spin waves (magnons), such that transitions between its energy levels (magnon number states) correspond to highly directional (superradiant) photon emission or absorption [4-12].
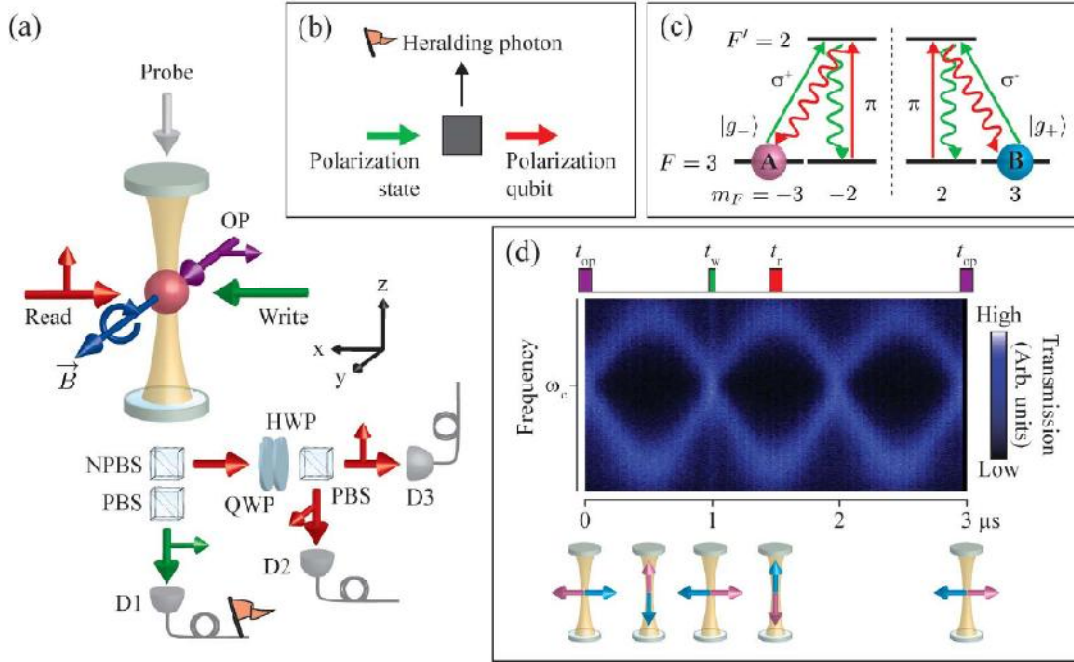
We have demonstrated a heralded quantum memory [3], i.e., system where a single photon announces polarization storage in the form of a single collective-spin excitation (magnon) that is shared between two spatially overlapped atomic ensembles. The heralded storage occurs rarely (p ~ 10^{-6} in our non-optimized setup), but when it does, the incident photon is stored and can later be recreated with good efficiency ($\varepsilon \geq$ 50%) and sub-Poissonian statistics ($g_2 = 0.24$), while the photon polarization state is restored with very high fidelity (F > 90%).

Heralded storage is achieved by means of a spontaneous Raman process that simultaneously creates a photon of fixed polarization (that serves as the herald), and a magnon that is a copy of the input-beam polarization. To store an arbitrary polarization state

$$|\Phi\rangle = sin\theta|R\rangle + e^{-i\phi_f}cos\theta|L\rangle, \qquad (1)$$

written as a superposition of two right/left circularly polarized states $|R\rangle$, $|L\rangle$ with two arbitrary angles θ, ϕ, we use two spatially-overlapped atomic ensembles A, B inside an optical resonator (Fig. V1). The atomic levels are chosen such that ensemble A (B) absorbs only right (left) circularly polarized light, while both can emit a photon of the same polarization (π) into the resonator on the Raman transition of interest (Fig. V1). The detection of the emitted π photon heralds the mapping of the input polarization state onto

a magnon, but does not provide "which-path" information to distinguish between *A* and *B*. The heralding also ensures that, even if the input is a coherent beam, only one magnon is generated between the two ensembles in the limit of small Raman scattering probability.
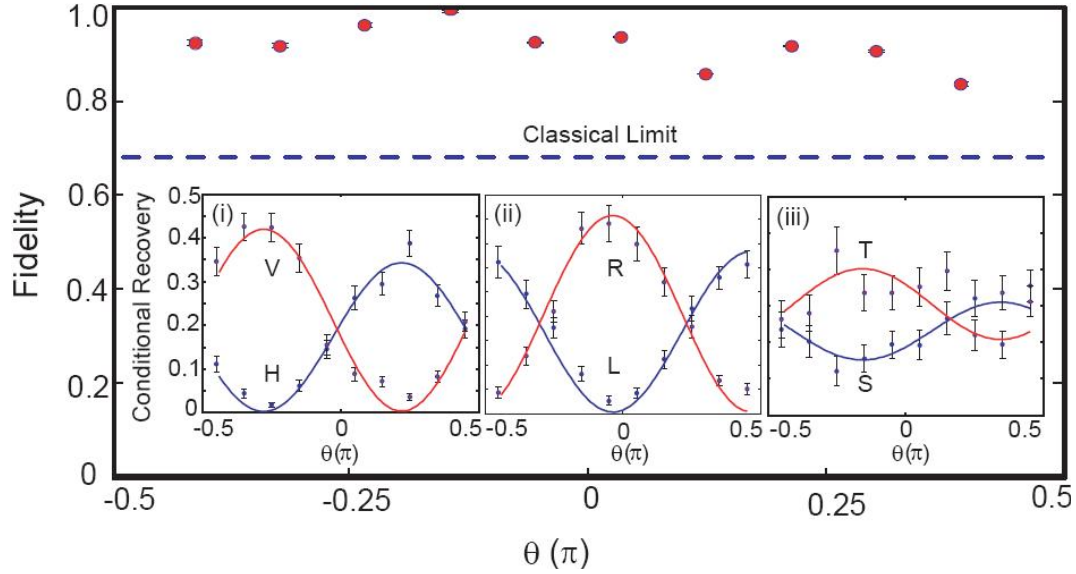

Figure V1. (a) Setup. Small arrows indicate beam polarization, OP is the optical pumping beam. NPBS, PBS, QWP, and HWP denote a non-polarizing beamsplitter, a polarizing beamsplitter, a quarter-waveplate, and a half-waveplate, respectively. D1, D2, D3 are single-photon counting modules. A static magnetic field produces magnon precession. **(b) Basic idea of the heralded storage.** A heralding photon of fixed polarization announces the storage of a photon of arbitrary, and potentially unknown polarization, in the atomic ensemble. **(c) Energy levels.** Ensembles *A* and *B* are initially prepared in $|g\pm\rangle=|F=3,m_F=\pm3\rangle$. The write (green) and the read (red) processes are $\sigma^\pm-\pi$ and $\pi-\sigma^\pm$ spontaneous Raman transitions, respectively. **(d) Precession of the two macroscopic spins**, as measured by cavity transmission spectroscopy, and timing of the optical pumping (t_{op}), write (t_w), and read (t_r) processes.

The "write" process thus projects the polarization state $|\psi*$ onto a magnon superposition state

$$|\Psi\rangle = sin\theta|1\rangle_A|0\rangle_B + e^{-i\phi_f}cos\theta|0\rangle_A|1\rangle_B, \ (2)$$

where $|n\rangle_k$ denotes *n* magnons in ensemble *k* (*k* = *A*, *B*). For general input polarization, this process creates an entangled state of the two ensembles. At a later time, the stored state can be retrieved on demand as a single photon by utilizing the strong coupling

[4,12] of the magnon to the resonator mode ("read" process). The heralding serves to enhance the fidelity of the write process by announcing successful events. While the storage probability is low in our present setup, whenever there is a heralding event, a single magnon corresponding to the input-field polarization is stored with high fidelity. The single-photon nature of the retrieved field is confirmed by a conditional autocorrelation measurement indicating four-fold suppression of two-photon events compared to a Poissonian source ($g_2 = 0.24(5)$). The heralding process may thus be alternatively viewed as a quantum non-demolition measurement of a single photon which preserves the polarization, and stores the photon.

Figure V2. Polarization fidelity of the stored photon as a function of θ for $\phi=0$ (Eq. 1). The dashed line indicates the classical limit of 2/3. Insets (i)-(iii): The results of projection measurements of the output field in three mutually-orthogonal bases, H-V, L-R, and S-T. The solid curves are a simultaneous fit for all sixty data points. The error bars represent statistical errors due to finite detection counts. No backgrounds have been subtracted.

To investigate the quality of the heralded polarization memory, we evaluate the polarization fidelity of the retrieved single photon with respect to the input state. We determine the density matrix ρ_{meas} of the output polarization by measuring the projection onto three polarization bases: $|R\rangle\pm|L\rangle$ (H-V), $|R\rangle$ and $|L\rangle$ (L-R), and $|R\rangle\pm i|L\rangle$ (S-T). As the phase θ of the input state Eq. (1) is varied, the projection onto those bases displays a sinusoidal variation as expected (inset of Fig. V2). The polarization fidelities F of the retrieved single photons for the ten states shown in Fig. V2 as well as for the six fiducial

input states, H, V, L, R, S, and T are evaluated from the measured density matrices. Fig. V2 shows that F is close to unity with no notable dependence on the zenith angle θ, and we have verified separately that the same is true for the azimuth angle ϕ. In particular, for any of the six fiducial states the measured fidelity F without any background subtraction is significantly above the classical limit of 2/3 for state-independent storage.

We also estimate the degree of entanglement present between samples A and B during storage. The amount of entanglement may be quantified by the concurrence C [14], where $1 \geq C > 0$ indicates entanglement. The concurrence of an atomic state C is bounded by that of the corresponding photonic state C_{ph} as discussed in the Supplementary Information of Ref. [13]. C_{ph} is observed to vary with zenith angle θ, as expected, with a maximum value of $C_{ph} = 0.034(4)$ for the $|H\rangle = |R\rangle + i|L\rangle$ state.
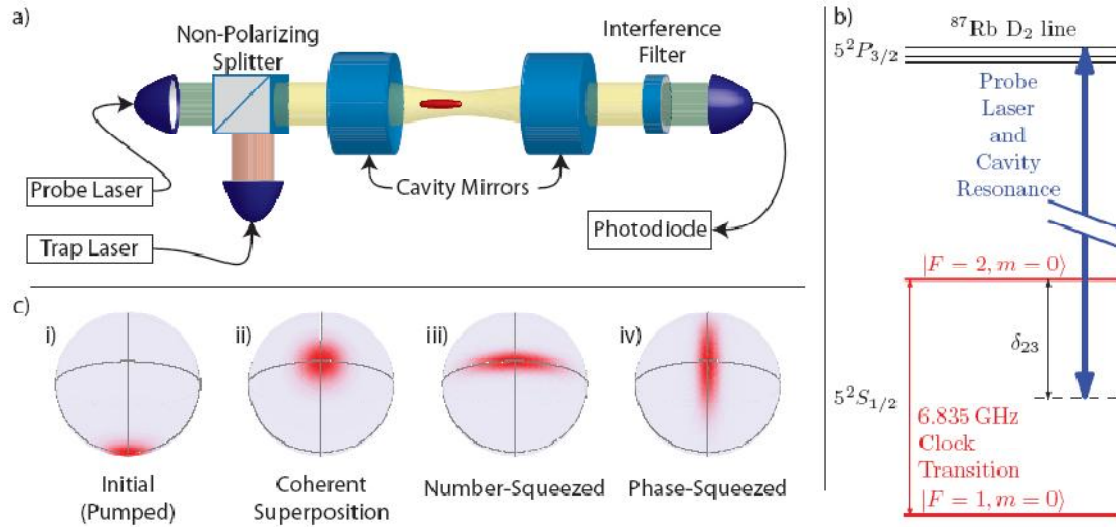
The low success probability may be improved upon by a dipole trap and a modified resonator, which will realistically increase the transverse optical depth to unity, and the single-atom cooperativity in the cavity mode to 0.1, respectively. The success probability and the effective success rate will then be ~1% and ~200 s^{-1}, respectively. The retrieved photons in this scheme have controllable waveforms, and can easily be interfered with one another with high fringe contrast because of their narrow, nearly Fourier-limited bandwidth [10]. This is a crucial feature for any quantum information application. Furthermore, by applying this scheme to photons of undetermined polarization from a probabilistic source of entangled-photon pairs, it should be possible to realize a heralded source of high-quality entangled-photon pairs for various tasks in quantum information processing.

6. Generation of states with reduced quantum uncertainty for an atomic clock

Atomic clocks are the most accurate instruments ever developed. For clocks that operate with an atomic ensemble to improve the signal over that for a single particle, the precision is fundamentally limited by the projection noise associated with the uncorrelated random measurement outcomes for the individual particles [15-17], a situation referred to as the standard quantum limit (SQL). However, it is possible to induce
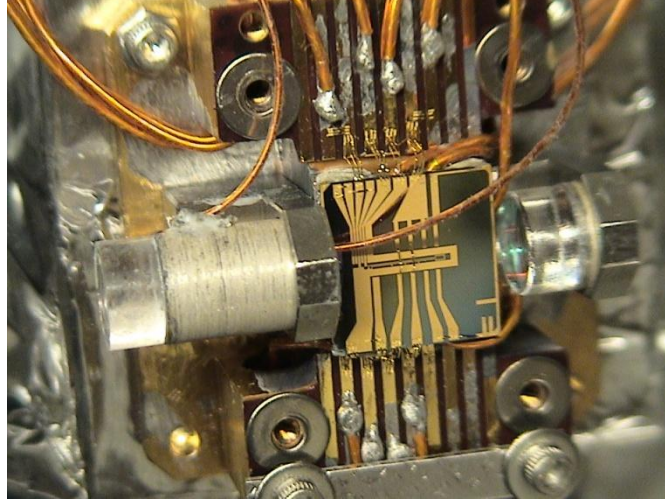
quantum mechanical correlations (entanglement) between the particles to generate reduced-uncertainty states ("squeezed states") that overcome the SQL [18-20].

Figure V3. Measurement-induced pseudo-spin squeezing on an atomic clock transition. (a) Setup. A laser-cooled ensemble of [87]Rb atoms is loaded into a far-detuned optical dipole trap inside an optical resonator. The ensemble can be prepared in a superposition of hyperfine clock states $|1\rangle=|F=1,m_F=0\rangle$, $|2\rangle=|F=2,m_F=0\rangle$ by microwave pulses. A population difference N produces a resonator frequency shift that is measured with a probe laser. **(b) Atomic level structure.** The resonator is tuned such that atoms in the two clock states produce equal and opposite resonator frequency shifts via the state-dependent atomic index of refraction. **(c) Preparing a squeezed input state for an atomic clock.** A number-squeezed state (iii) can be generated from an unentangled state (coherent spin state, CSS) along x (ii) by measurement of N. It can then be rotated by a microwave pulse into a phase-squeezed state (iv), allowing a more precise determination of the phase acquired in the free evolution time of the atomic clock.

A two-level system can be formally described as a (pseudo-)spin $s=1/2$. In a typical precision experiment, the energy difference between the two levels is measured as a quantum mechanical phase accumulated in a given time. The result is read out as a population difference that can be formally viewed as the z-component S_z of the ensemble spin vector, where the sum is over the individual particles. The projection noise ΔS_z can be reduced by entanglement [16-19], by redistributing quantum noise from the S_z spin component to another spin component that is not directly affecting the experiment precision ("spin squeezing" [18-20]).
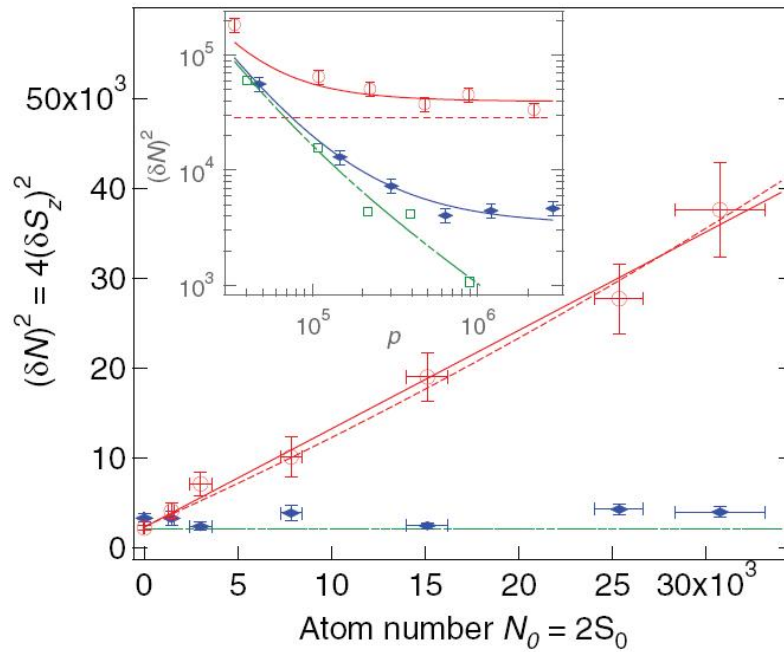
Figure V4. Microfabricated chip with mounted optical resonator. The resonator mode is aligned 200 μm above the surface of the microchip. The left mirror is mounted on a piezoceramic tube for tuning of the resonance frequency. The resonator finesse is $F=8000$.

For an ensemble spin vector S oriented along the x axis, a state is spin squeezed [20] along the z-direction (or "number squeezed") if the uncertainty ΔS_z obeys $(\Delta S_z)^2 < |\langle S_x \rangle|/2$. For a maximally coherent system with $|\langle S_x \rangle| \approx S_0$, where $S_0 = N_0/2$ is the maximum possible spin of the ensemble containing N_0 particles, spin squeezing corresponds to a situation where the variance $(\Delta N)^2$ of the population difference $\Delta N = N_2 - N_1 = 2S_z$ between the two states $|1\rangle$, $|2\rangle$ is less than the projection noise limit, $(\Delta N)^2 < N_0$. However, since in real systems coherence (i.e. interference contrast) is often reduced, such that $|\langle S_x \rangle| < S_0$, spin-noise suppression below the projection noise limit $(\Delta S_z)^2 < |\langle S_x \rangle|/2$ is only a necessary but not a sufficient condition for spin squeezing. Thus to demonstrate spin squeezing one must measure both the spin noise ΔS_z, and the magnitude of the spin vector $|S|$.

Spin squeezing requires an interaction between the particles [20] that can be achieved by collective coupling of the ensemble to a light field [21], provided the sample's optical depth (opacity if probed on resonance) is sufficiently large. Under appropriate conditions, the light-atom interaction entangles the ensemble spin S with the electromagnetic field, and a subsequent field measurement can then project the atomic ensemble into a spin-squeezed state [16-21]. Such conditionally spin-squeezed input
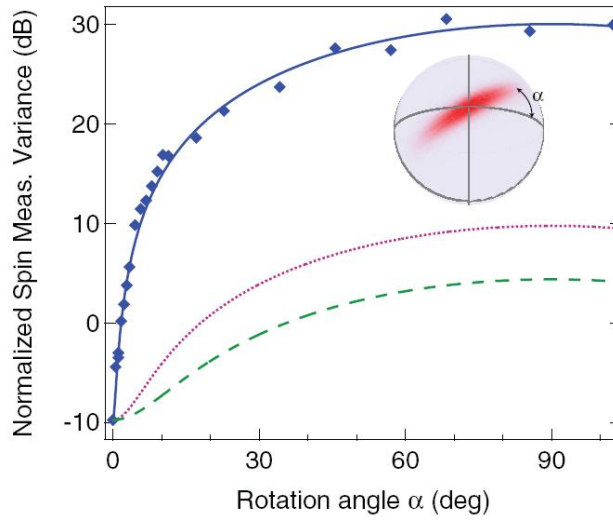
states can improve the sensitivity of a precision measurement device such as an atomic clock.

To prepare a spin-squeezed input state to an atomic clock, we adapt the proposal by Kuzmich, Bigelow, and Mandel [21] for a quantum non-demolition (QND) measurement of Sz with far off-resonant light [22]. An ensemble of up to 10^5 laser-cooled ^{87}Rb atoms is optically trapped inside an optical resonator that serves to enhance the signal and optical depth (Fig. V4). One resonator mode is tuned such that the state-dependent atomic index of refraction produces a mode frequency shift that is proportional to the population difference $N = N_2 - N_1 = 2S_z$ between the hyperfine clock states $|1\rangle = |5S_{1/2}, F=1, m_F=0\rangle$ and $|2\rangle = |5S_{1/2}, F=2, m_F=0\rangle$. Then a QND measurement of S_z can be performed by measuring the transmission of a weak probe beam through the ensemble-resonator system. A frequency stabilization system for probe laser and resonator ensures that the probe transmission noise is close to the photocurrent shot-noise limit.

Figure V5. Projection noise limit and spin noise reduction. The measured spin noise for an uncorrelated state (CSS, open red circles) agrees with the theoretical prediction $(\Delta S_z)^2 = S_0/2$, with negligible technical noise (solid and dashed red lines). Our measurement of S_z at photon number $p = 5 \times 10^5$ has an uncertainty $(\delta S_z)^2$ (solid blue diamonds) substantially below the SQL. Inset: Dependence of spin measurement $(\delta S_z)^2 = (\delta N)^2/4$ on probe photon number p for $N_0 = 3 \times 10^4$. With increasing photon number, the measurement uncertainty (solid blue diamonds) drops below the projection noise level (dashed red line). Also shown is the technical noise without atoms expressed as an equivalent spin noise (open green squares).

Fig. V5 shows the projection noise for an unentangled state of uncorrelated atoms (coherent spin state, CSS), and the quantum noise for a conditionally prepared entangled state with a random, but known value of S_z. For the former (red data points) the linear dependence of $(\Delta S_z)^2$ on total atom number N_0 shows that we have prepared a state at the projection noise limit. For the latter, at low atom number the measurement noise exceeds the SQL due to photon shot noise and some technical noise (dash-dotted green line in Fig. V5), while at higher atom number $N_0 = 3 \times 10^4$ we achieve a 9 dB suppression of spin noise below the SQL.

Figure V6. Shape of the squeezed uncertainty region. A rotation about the mean spin vector $\langle \boldsymbol{S} \rangle$ is applied between the first and second spin measurements. The spin noise reduction along z ($\alpha=0$) below the projection noise limit is accompanied by a substantial spin noise increase in the equatorial plane ($\alpha=\pi/2$). The solid blue line corresponds to an elliptic shape of the uncertainty region. The dotted magenta line would correspond to a state at the Heisenberg limit in the ideal case where the measurement does not reduce the length of the spin vector $|\boldsymbol{S}|$. The dashed green line is the true Heisenberg limit for our measurement, taking into account the reduction of $|\boldsymbol{S}|$.

The reduction of ΔS_z below the SQL is accompanied by a substantial increase in ΔS_y. The shape of the uncertainty region can be verified by rotating the state prepared by the squeezing pulse by a variable angle about $\langle \boldsymbol{S} \rangle$ before performing the second S_z measurement. The variance $(\Delta S_\alpha)^2$ thus obtained is displayed in Fig. V6. The data are well described by a model that assumes the spin noise after the first measurement to constitute an ellipse with its short axis along z (solid blue line). The uncertainty area $A = \Delta S_z\, \Delta S_y$ is well above the Heisenberg limit $A_H = |\boldsymbol{S}|\, /2$ (dashed green line). The larger

uncertainty is primarily due to the atomic-projection-noise-induced resonator shift, which produces fluctuations in probe transmission well above the photon shot noise limit, resulting in substantial differential light shifts between the clock states. This effect, though not currently a limitation on our squeezing performance, can be reduced in future experiments by measuring on cavity resonance, or by using a feedback technique that keeps the transmitted photon number constant.
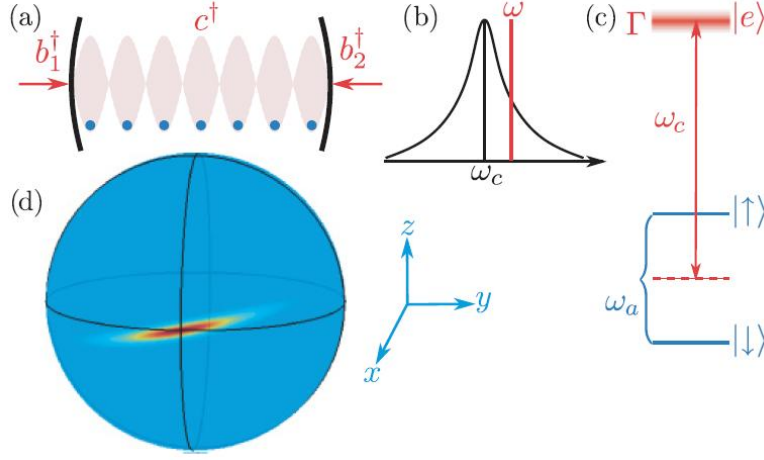
When we compare the observed squeezing to the reduction of clock signal $|S|$, measured via the clock fringe contrast, we find that we achieve 4dB of spin squeezing [20], and 3dB of improvement in clock signal-to-noise ratio over the standard quantum limit [16,17]. The contrast loss is not fundamental, and in part simply limited by the detuning and intensity of the light used to stabilize the resonator length. We are currently making modifications to the setup to reduce this technical noise. If successful, the improvement in signal-to-noise ratio should allow us to obtain an improvement over the SQL that matches the observed spin noise reduction of 9dB. If technical noise can be suppressed further, a fundamental limit associated with scattering into free space is set by the optical depth OD of the sample [19], which for our present parameters (OD $\approx 5 \times 10^3$) would amount to ~18 dB of spin squeezing.

7. Deterministic spin squeezing by cavity feedback

We have proposed and demonstrated a new a cavity feedback method for deterministic production of squeezed spin states [31–38] using light-mediated interactions between distant atoms in an optical resonator. This approach generates spin dynamics similar to those of the one-axis twisting Hamiltonian $H = S_z^2$ in the original proposal of Kitagawa and Ueda [31]. Cavity squeezing scales to a much higher particle number than direct manipulation of ions [39] and employs dilute ensembles rather than dense condensates of interacting atoms [40]. Unlike measurement-based squeezing [41,42], it unconditionally produces a known squeezed state independent of detector performance.

We have implemented cavity squeezing for the canonical $|F = 1, m_F = 0\rangle$ to $|F = 2, m_F = 0\rangle$ hyperfine clock transition in ^{87}Rb atoms, achieving a 5.6(6) dB improvement in signal-to-noise ratio [32,33]. To our knowledge, this is the largest such improvement to date. Moreover, the shape and orientation of the uncertainty regions we observe agree

with a straightforward analytical model [43], without free parameters, over two orders of magnitude in effective interaction strength.
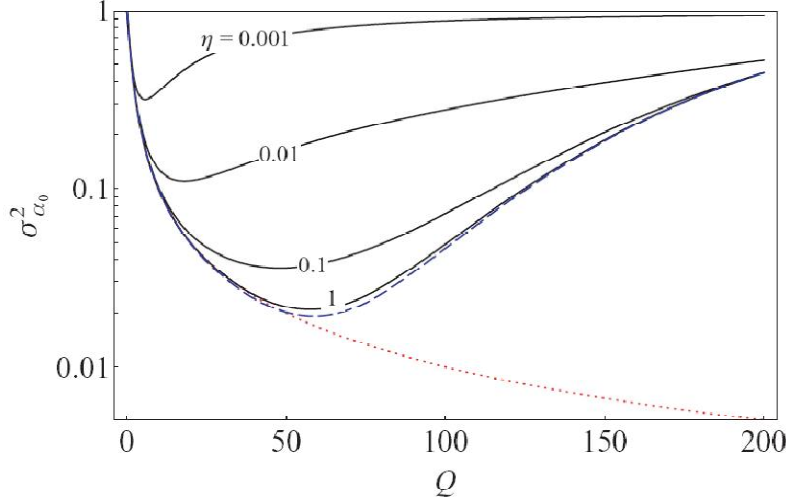

Figure V7. Scheme for spin squeezing by cavity feedback. An ensemble of atoms is uniformly coupled to a laser field in an optical resonator (a). A laser tuned to the slope of a cavity resonance (b), at equal and opposite detunings from transitions $|\uparrow\rangle \rightarrow |e\rangle$ and $|\downarrow\rangle \rightarrow |e\rangle$ (c), shears a coherent spin state prepared along the *x* axis into a squeezed spin state (d), illustrated by a tomographic probability distribution on the Bloch sphere.

For an ensemble of two-level (spin-1/2) atoms, described by a collective spin S, the squeezing is produced by an ensemble-light interaction Hamiltonian of the form $c^\dagger c S_z$ that represents the differential energy shift between the two atomic states due to the intracavity light with photon number $c^\dagger c$. This photon number depends on the population difference $2S_z$ between the atomic states because the precise tuning of the resonator mode relative to the driving laser depends on the atoms' state-dependent index of refraction. In particular, if $c^\dagger c$ depends linearly on S_z, the differential energy shift causes a precession of the spin vector about the z axis at a rate proportional to S_z, similar to the dynamics of a Hamiltonian $\propto S_z^2$ [32]. The initially circular uncertainty region of a CSS is then sheared into an ellipse (Fig. V7d) that is narrower in one direction than the original CSS, corresponding to spin squeezing. The spin correlations between different atoms arise from the fact that the phase between the two states in any individual atom now depends on the state population difference $2S_z$ of the entire ensemble.

The shearing strength $Q = Sp\phi^2$ is a dimensionless measure of the light-mediated interaction strength, where S is the collective atomic spin, p is the photon number transmitted through the resonator (Figure V7), and ϕ is the spin precession angle per

photon transmitted through the resonator. Figure V8 shows the calculated minimum variance, normalized to the standard quantum limit (projection noise limit) as a function of shearing strength Q for various values of the cooperativity η [43]. The parameters $\eta = 0.1$, $S=10^4$ are similar to those used to achieve squeezing in Refs. [44,45].
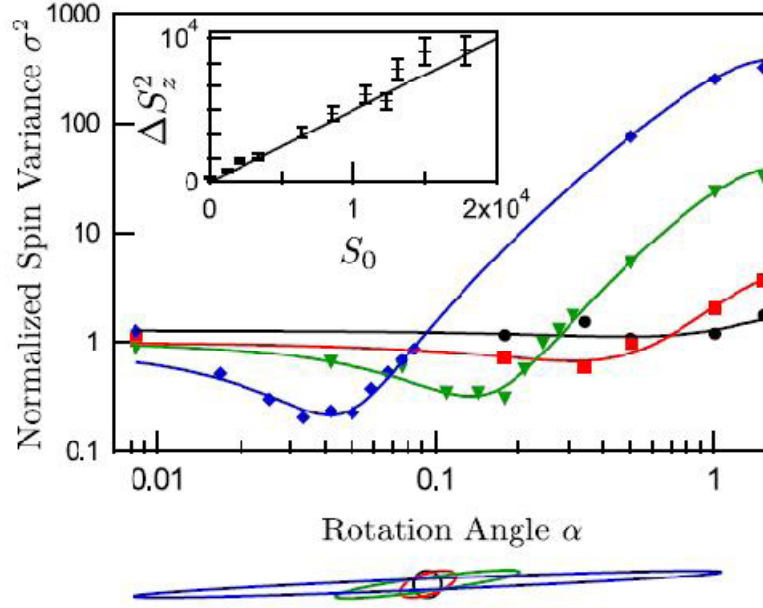

Figure V8. Theoretically attainable cavity squeezing. Minimum variance σ^2 (normalized to the standard quantum limit) as a function of shearing strength Q for $S=10^4$ and various single-atom cooperativities η = 0.001, 0.01, 0.1, 1 (solid lines). The dashed line shows the limit due to the curvature of the Bloch sphere when free-space scattering is ignored. The dotted line shows the variance neglecting both free-space scattering and curvature, scaling as $1/Q$ for $Q \gg 1$.

We observe the shearing by rotating the state through an angle α with a microwave pulse about the axis of its mean spin vector and recording the variance ΔS_α^2 of a subsequent measurement of S_z over a series of 100 identical preparations. The measured variance is normalized to projection noise, based on a first-principles calculation using accurately measured cavity parameters [45]. The inset of Fig. V9 shows the observed ΔS_z^2 of the initial spin state as a function of atom number $2S_0$, as well as the calculated projection noise limit.

Typical data of ΔS_α^2 are displayed in Fig. V9. As the state is rotated the variance dips below projection noise as the minor axis of the ellipse is aligned with z and then increases beyond it as the major axis in turn rotates towards z. The variation of ΔS_α^2 with angle is sinusoidal with a period π, as it must be for any distribution of S_y-S_z fluctuations. We record such curves over a range of photon numbers, corresponding to increasing shearing strength Q, keeping the effective atom number constant at $2S_0= 3\times10^4$. We

compare the fitted phase and minimum and maximum variance of each sinusoid to the predictions of our model [43], finding good agreement.
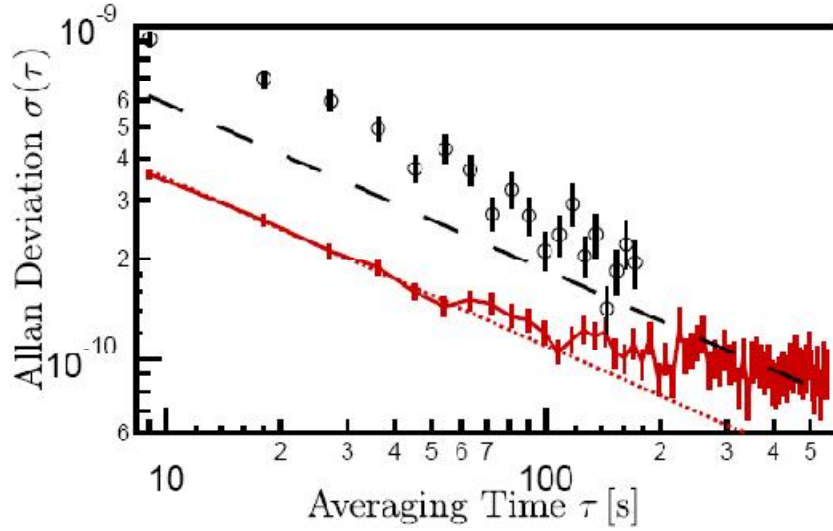

Figure V9. **Shape of squeezed uncertainty regions.** Normalized variance σ^2 as a function of rotation angle α about the mean spin direction for states prepared with shearing $Q=0$ (black circles), $Q=1.2$ (red squares), $Q=7.7$ (green triangles), and $Q=30.7$ (blue diamonds). The curves are cosine fits. Statistical error bars are comparable to the symbol size. The shapes of the corresponding uncertainty regions are illustrated below the plot. Inset: Observed variance ΔS_z^2 of the initial state as a function of S_0. The line is the projection noise limit as determined from cavity parameters.

For 3×10^4 atoms and $Q=19$, we reduce the spin noise by 6.7(6)dB. At this photon number our contrast is $C=0.78(2)$, so that we demonstrate a 5.6(6)dB improvement in potential measurement precision over that of the initial uncorrelated state. By subtracting our independently measured readout noise, we infer that states prepared by a shearing $Q=19$ have an intrinsic spin variance that is a full 10(1) dB below the projection noise limit. Such states, when used as input states to a Ramsey type atomic clock, should allow clock operation below the standard quantum limit.

8. Squeezed atomic clock and orientation-dependent lifetime of spin-squeezed states

We have investigated the lifetime of spin squeezed states and have shown that for an atomic clock in which the dominant environmental perturbation is phase noise, the squeezed-state lifetime varies by an order of magnitude depending on whether the squeezed variable is the phase (subject to environmental perturbation) or the (essentially unperturbed) population difference between states. We have used the spin squeezed states as prepared by cavity feedback squeezing [43,44] as input states to an atomic clock. We demonstrate a clock with a phase- squeezed input state whose precision exceeds the standard quantum limit, and present the first measurement of such a clock's Allan deviation spectrum (Fig. V10). The clock reaches a given precision 2.8(3) times faster than the standard quantum limit for integration times up to 50 s.

Figure V10. Allan deviation of a squeezed clock. The solid red line with error bars was measured using a squeezed input state. The dotted red line indicates $\sigma(\tau) = 1.1 \times 10^{-9} \ s^{1/2}/\tau^{1/2}$. The open black circles were measured with a traditional clock using an uncorrelated input state. The dashed black line at $1.85 \times 10^{-9} \ s^{1/2}/\tau^{1/2}$ indicates the standard quantum limit at 100% signal contrast.

As a demonstration, we have operated such a clock with a Ramsey interrogation time $T_R = 200$ μs, short enough that the classical frequency noise in our system does not destroy the phase squeezing. The effective atom number was $2S0 = 3.5 \times 104$, the clock cycle time was 9 s and the signal contrast was C = 81%. Only a single Ramsey

interrogation was performed for each MOT loading cycle, giving a duty factor of 2×10^{-5}. The result is the first measurement of Allan deviation [2] for an atomic clock operating beyond the SQL, including all noise and slow drifts (Fig. 3, red solid line). For comparison, we also evaluate a clock operated with an uncorrelated input state close to a CSS, 100(2)% signal contrast and otherwise identical parameters (Fig. 3, black circles). An ideal projection-noise-limited clock with the same atom number, interrogation time and duty factor could reach a stability $\sigma(\tau) = 1.85 \times 10^{-9}$ $s^{1/2}/\tau^{1/2}$ (Fig. 3, dashed black line). At short times our squeezed- state clock reaches a fractional frequency uncertainty of $\sigma(\tau) = 1.1 \times 10^{-9}$ $s^{1/2}/\tau^{1/2}$. At longer times we reach a noise floor at 10^{-10} fractional stability (0.7Hz absolute stability) due to slow drifts of the magnetic field in our apparatus.

If the classical frequency noise could be controlled at the level of 100 µHz, perhaps by operating in a magnetic trap at the magic bias field of 3.23G, the squeezed lifetime could be extended sufficiently to allow a squeezed clock to operate with a Ramsey precession time of one second, as demonstrated by Treutlein et al. on a microchip similar to the one used in the present experiment [24]. Even without improvements to our squeezedstate preparation or 9 s cycle time, this could yield a short-term stability of $\sigma(\tau) = 2 \times 10^{-13}$ $s^{1/2}/\tau^{1/2}$, competitive with the stability of current fountain clocks [56].

9. Strongly coupled resonator for ensemble cavity QED

We have built a system where an atomic ensemble can be placed inside an optical resonator that is strongly coupled to a single atom. This system is similar to those used for cavity QED studies as pioneered by Kimble and Rempe, but unlike those systems the resonator is macroscopic, allowing a cesium magneto-optical trap to be placed inside the resonator. Fig. V10 shows the setup. The maximum cavity cooperativity for an atom at an antinode on the cavity axis is h=8>1, placing the system into the strong-coupling regime.

Possible future experiments include the quantum non-demolition measurement of a photon where an incident photon is stored in the ensemble via electromagnetically induced transparency as a spin-wave excitation, and that spin wave excitation detected non-destructively via a measurement of the cavity transmission. The stored photon can

then be recovered at a later time while information about its presence is available. Such a system could be used for many applications, including the generation of entangled photons on demand.
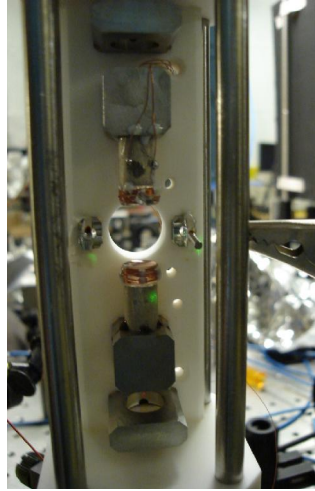

Fig. V10. Setup with macroscopic cavity strongly coupled to a single atom. The spacing between the resonator mirrors mounted on piezoceramic tubes for cavity tuning is ~1cm, so that a magneto-optical trap can be operated inside the resonator. Two aspheric lenses (left and right near cavity center) allow the focusing of a transverse beam to 2 μm for atom probing or single-atom trapping.

We have recently demonstrated that we can make atom-number resolving measurements using transmission through the resonator. In a histogram of the transmitted photon number (with an average photon number of typically 100 transmitted through an empty cavity) we can identify peaks corresponding to zero, one, two, and three atoms in the resonator. This is promising for a future demonstration of a photon-number resolving detector that operates by mapping an input state of the light field via electromagnetically induced transparency onto a spin wave excitation in the ensemble, and detecting the number of atoms transferred between hyperfine states in the atom-photon mapping.

References

[1] D.N. Matsukevich and A. Kuzmich, "Quantum State Transfer Between Matter and Light," Science **306**, 663-666 (2004).
[2] K.S. Choi and H. Deng and J. Laurat and H.J. Kimble, "Mapping photonic entanglement into and out of a quantum memory," Nature **452**, 67-71 (2008).
[3] H. Tanji, S. Ghosh, J. Simon, B. Bloom, and V. Vuletic, "Heralded single-magnon quantum memory for photon polarization states," submitted to Phys. Rev. Lett. (8/2008), quant-ph/0808.3603.

[4] L.-M. Duan, M. D. Lukin, J. I. Cirac, and P. Zoller, "Generation of nonclassical photon pairs for scalable quantum communication with atomic ensembles", Nature **414**, 413 (2001).

[5] Kuzmich, W. P. Bowen, A. D. Boozer, A. Boca, C. W. Chou, L.-M. Duan, and H. J. Kimble, "Generation of nonclassical photon pairs for scalable quantum communication with atomic ensembles", Nature **423**, 731 (2003).

[6] H. van der Wal, M. D. Eisaman, A. Andre, R. L. Walsworth, D. F. Phillips, A. S. Zibrov, and M. D. Lukin, "Atomic Memory for Correlated Photon States", Science **301**, 196 (2003).

[7] C. W. Chou, H. de Riedmatten, D. Felinto, S. V. Polyakov, S. J. van Enk and H. J. Kimble, "Measurement-induced entanglement for excitation stored in remote atomic ensembles", Nature **438**, 828 (2005).

[8] T. Chanelière, D. N. Matsukevich, S. D. Jenkins, S.-Y. Lan, T. A. B. Kennedy and A. Kuzmich, "Storage and retrieval of single photons transmitted between remote quantum memories", Nature **438**, 833 (2005).

[9] M. D. Eisaman, A. André, F. Massou, M. Fleischhauer, A. S. Zibrov and M. D. Lukin, "Electromagnetically induced transparency with tunable single-photon pulses", Nature **438**, 837 (2005).

[10] J. K. Thompson, J. Simon, H. Loh, and V. Vuletic, "A High-Brightness Source of Narrowband, Identical-Photon Pairs," Science **303**, 74-77 (2006).

[11] A.T. Black, J. K. Thompson, and V. Vuletic, "On-Demand Superradiant Conversion of Atomic Spin Gratings into Single Photons with High Efficiency," Phys. Rev. Lett. **95**, 33601 (1-4) (2005).

[12] J. Simon, H. Tanji, J. K. Thompson, and V. Vuletic, "Interfacing Collective Atomic Excitations and Single Photons," Phys. Rev. Lett. **98**, 183601 (1-4) (2007).

[13] J. Simon, H. Tanji, S. Ghosh, and V. Vuletic, "Single-Photon Bus between Spin-Wave Quantum Memories," Nature Physics **3**, 765-769 (2007).

[14] W. K. Wootters, "Entanglement of Formation of an Arbitrary State of Two Qubits," Phys. Rev. Lett. **80**, 2245-2248 (1998).

[15] G. Santarelli, Ph. Laurent, P. Lemonde, A. Clairon, A. G. Mann, S. Chang, A. N. Luiten, and C. Salomon, "Quantum Projection Noise in an Atomic Fountain: A High Stability Cesium Frequency Standard," Phys. Rev. Lett. **82**, 4619-4622 (1999).

[16] D. J. Wineland, J. J. Bollinger, W. M. Itano, F. L. Moore, D. J. Heinzen, "Spin squeezing and reduced quantum noise in spectroscopy," Phys. Rev. A **46**, R6797 (1992).

[17] D. J. Wineland, J. J. Bollinger, W. M. Itano, D. J. Heinzen, "Squeezed atomic states and projection noise in spectroscopy," Phys. Rev. A **50**, R67 (1994).

[18] V. Meyer, M. A. Rowe, D. Kielpinski, C. A. Sackett, W. M. Itano, C. Monroe, and D. J. Wineland, "Experimental Demonstration of Entanglement-Enhanced Rotation Angle Estimation Using Trapped Ions," Phys. Rev. Lett. **86**, 5870-5873 (2001).

[19] D. Leibfried, M.D. Barrett, T. Schaetz, J. Britton, J. Chiaverini, W.M. Itano, J.D. Jost, C. Langer, and D. Wineland, "Toward Heisenberg-Limited Spectroscopy with Multiparticle Entangled States," Science **304**, 1476 (2004).

[20] M. Kitagawa and M. Ueda, "Squeezed spin states," Phys. Rev. A **47**, 5138 (1993).

[21] A. Kuzmich, N. P. Bigelow, and L. Mandel, "Atomic quantum non-demolition measurements and squeezing," Europhys. Lett. **42**, 481-486 (1998).

[22] A. Kuzmich, L. Mandel, N. P. Bigelow, "Generation of Spin Squeezing via Continuous Quantum Nondemolition Measurement," Phys. Rev. Lett. **85**, 1594-1597 (2000).

[23] C. Petitjean, D.V. Bevilaqua, E. J. Heller, and P. Jacquod, "Displacement Echoes: Classical Decay and Quantum Freeze", Phys. Rev. Lett. **98**, 164101.

[24] S. Wu, W. Rooijakkers, P. Striehl, M. Prentiss, Phys. Rev. A **70**, 013409 (2004).

[25] G.-B. Jo et al., Phys. Rev. Lett. **98**, 030407 (2007).

[26] S. Wu, E. Su, M. Prentiss, Phys. Rev. Lett. **99**, 173201 (2007).

[27] T. Lahaye et al., Phys. Rev. A **74**, 033622 (2006).

[28] W. Hansel et al., Phys. Rev. Lett. **86**, 608 (2001).

[29] P. Striehl, Ph.D. thesis, Harvard Univ. (2007).

[31] M. Kitagawa and M. Ueda, Phys. Rev. A **47**, 5138 (1993).

[32] D. J. Wineland, J. J. Bollinger, W.M. Itano, F. L. Moore, and D. J. Heinzen, Phys. Rev. A **46**, R6797 (1992).

[33] D. J. Wineland, J. J. Bollinger, W.M. Itano, and D. J. Heinzen, Phys. Rev. A **50**, 67 (1994).

[34] A. S. Sørensen and K. Mølmer, Phys. Rev. Lett. **86**, 4431 (2001).

[35] A. Sørensen, L.-M. Duan, J. I. Cirac, and P. Zoller, Nature (London) **409**, 63 (2001).

[36] A. Kuzmich, N. P. Bigelow, and L. Mandel, Europhys. Lett. **42**, 481 (1998).

[37] A. Kuzmich, L. Mandel, and N. P. Bigelow, Phys. Rev. Lett. **85**, 1594 (2000).

[38] T. Takano, M. Fuyama, R. Namiki, and Y. Takahashi, Phys. Rev. Lett. **102**, 033601 (2009).

[39] V. Meyer, M.A. Rowe, D. Kielpinski, C. A. Sackett,W. M. Itano, C. Monroe, and D. J. Wineland, Phys. Rev. Lett. **86**, 5870 (2001).

[40] J. Esteve, C. Gross, A. Weller, S. Giovanazzi, and M. K. Oberthaler, Nature (London) **455**, 1216 (2008).

[41] M. H. Schleier-Smith, I. D. Leroux, and V. Vuletic, Phys. Rev. Lett. **104**, 073604.

[42] J. Appel, P. J. Windpassinger, D. Oblak, U. B. Hoff, N. Kjærgaard, and E. S. Polzik, Proc. Natl. Acad. Sci. U.S.A. **106**, 10 960 (2009)

[43] M. Schleier-Smith, I.D. Leroux, and V. Vuletic, Phys. Rev. A **81**, 021804(R) (2010).

[44] I.D. Leroux, M. Schleier-Smith, and V. Vuletic, Phys. Rev. Lett. **104**, 073602 (2010); selected as Editors' Suggestion.

[45] M. H. Schleier-Smith, I.D. Leroux, and V. Vuletic, Phys. Rev. Lett. **104**, 073604 (2010).

[46] J. H. T. Burke et al., Phys. Rev. A **78**, 023619 (2008).

[47] J. H. T. Burke et al., Phys. Rev. A **80**, 061603(R) (2009).

[48] N. H. Dekker et al., Phys. Rev. Lett. **84**, 1124 (2000).

[49] R. Folman et al., Adv.At. Mol. Opt. Phys. **48**, 263 (2002).

[50] J.-B. Trebbia et al., Phys. Rev. Lett. **98**, 263201 (2007).

[51] L. Cognet et al., Europhys. Lett. **47**, 538-544 (1999).

[52] D. W. Wang, M. D. Lukin and E. Demler, Phys. Rev. Lett. **92**, 076802 (2004).

[53] Y. J. Wang et al., Phys. Rev. Lett. **94**, 090405 (2005).

[54] A. Tonyushkin, S. Wu, and M. Prentiss, Phys. Rev. A **79**, 051402(R) (2009);

[55] S. Wu, A. Tonyushkin, and M. Prentiss, Phys. Rev. Lett. **103**, 034101 (2009).

[56] P. Treutlein, P. Hommelhoff, T. Steinmetz, T. W. Hänsch, and J. Reichel, Phys. Rev. Lett. **92**, 203005 (2004).